Matter and Radiation at Extremes REVIEW scitation.org/journal/mre

Recent progress on high-pressure and high-temperature studies of fullerenes and related materials

Cite as: Matter Radiat. Extremes 4, 028201 (2019); doi: 10.1063/1.5086310
Submitted: 1 August 2018 • Accepted: 30 October 2018 •
Published Online: 5 March 2019

Cuiying Pei and Lin Wang[a)]

AFFILIATIONS

Center for High Pressure Science and Technology Advanced Research (HPSTAR), 1690 Cailun Rd., Pudong District, Shanghai 201203, People's Republic of China

[a)] E-mail: wanglin@hpstar.ac.cn

ABSTRACT

Polymerization of fullerenes is an interesting topic that has been studied for almost three decades. A rich polymeric phase diagram of C_{60} has been drawn under a variety of pressure P and temperature T conditions. Knowledge of the targeted preparation and structural control of fullerene polymers has become increasingly important because of their utility in producing novel fullerene-based architectures with unusual properties and potential applications. This paper focuses on the polymeric phases of fullerenes and their derivatives under high P and/or high T. First, the polymerization behavior and the various polymeric phases of C_{60} and C_{70} under such conditions are briefly reviewed. A summary of the polymerization process of intercalated fullerenes is then presented, and a synthetic strategy for novel structural and functional fullerene polymers is proposed. Finally, on the basis of the results of recent research, a proposal is made for further studies of endohedral fullerenes at high P.

I. INTRODUCTION

Pressure is a fundamental thermodynamic variable that can dramatically alter the atomic and electronic structures of materials, resulting in concomitant changes to their properties.[1] The C=C bonds in fullerenes allow them to form covalent intermolecular bonds when treated at high pressure and high temperature (HPHT). The preparation path based on the reaction diagram and the treatment time greatly influences the completeness of transformation and the degree of polymerization. In addition, the hydrostatic nature of the compression environment plays an important role in bonding orientation and polymerization ordering. As a result, dimers, ordered one-dimensional (1D), 2D, and 3D polymers, and disordered graphite-like, diamond-like phases, etc., have been reported with a variety of novel polymerized fullerene architectures and a range of unusual properties and potential applications.[2–11]

The controllable polymerization of fullerenes to create new materials by using molecular confinement or co-intercalation by template molecules in the reactant has been extensively studied under a wide range of conditions of pressure P and temperature T. Solvated fullerenes, in which solvent molecules separate C_{60} and C_{70} molecules, are a series of crystalline materials with high stability, tunable metrics, and functionality. The intercalated solvent molecules play an important role in the construction of solvate lattices with different structures and further influence the phase transition at high P.[12–17] In addition, several metastable doped fullerene polymers have been synthesized under HPHT, such as C_{60}/Ni(OEP),[18,19] C_{60}/CNT,[20] and Na_4C_{60}.[21] The unique initial lattice structures and the different degrees of spatial confinement provided by the dopants lead to different polymeric phases accompanied by distinctive physical and electrical properties.

In 2001, Buga *et al.*[22] reported the P- and T-induced polymerization of the mono-atom endohedral fullerene La@C_{82} for the first time. Later, Liu and co-workers studied the structural transformations of Sm@C_{88} (Ref. 23) and solvated Sm@C_{90} (Ref. 24). The HOMO–LUMO gap decreased with increasing P until the carbon cage deformed, but no phase transition occurred. Pei *et al.*[25] observed for the first time that $Lu_3N@C_{80}$ underwent a reversible n- to p-type inversion under high pressure, with the p-type semiconductor being stable up to

25 GPa. The role of the intercage metal atom is to restrain the compression of the adjacent bonds and protect the endohedral fullerene against collapse, as well as decreasing and postponing the change in band gap. To date, however, the structure and properties of endohedral fullerenes under high P remain undefined.

This paper focuses on the properties and phases of fullerenes and their derivatives under HPHT. Four topics will be discussed: (i) how fullerenes are covalently incorporated into a polymer phase under HPHT; (ii) the correlation between the structural evolution and the novel properties of the polymeric phase; (iii) the effect of pressure on the polymerization behavior of doped or intercalated fullerenes; (iv) the polymeric fullerenes and their derivatives as new and versatile building blocks to prepare a wide variety of new fullerene-based materials governed by weak intermolecular interactions, showing unprecedented architectures and a wide range of potential applications.

II. HPHT RESEARCH ON C_{60}

To date, many different strategies have been exploited to prepare polymeric fullerenes. Chemical reactions can link C_{60} cages either covalently or supramolecularly, and the polymeric phases exhibit outstanding structural, electrochemical, and photophysical properties.[26] Photopolymerization,[27] pressure- and/or temperature-induced polymerization,[2–4] charge-transfer polymerization mediated by metals,[28] electron-beam-induced polymerization,[29] and plasma-induced polymerization[30,31] can be used to prepare novel polymeric fullerenes. In this section, we will present a general "panoramic" view of all-carbon polymeric fullerenes under high P and/or high T. Since the discovery of polymeric fullerene synthesized at high P in 1994,[32] there has been intense interest in the characterization of the polymeric phase products and in clarification of the mechanisms underlying the process of polymerization, because of the potentially useful physical, biological, and chemical properties of these products.[33,34] In particular, there have been extensive investigations of the influence of P and T treatment on polymerization,[35] on infrared spectroscopy (IR) and Raman vibrational properties,[36] and on photoluminescence[37] and magnetism.[38]

P-induced polymerization under various T and P has been studied extensively in recent years.[2] When moderate hydrostatic or quasi-hydrostatic P at high T is applied to pristine C_{60}, irreversible polymerization occurs over a limited range of T and P. As shown in the P vs. T phase diagram (Fig. 1), C_{60} polymers have orthorhombic, tetragonal, rhombohedral, or cross-linked phases. Recently, single crystals of these polymeric phases have been successfully prepared (the orthorhombic phase in Ref. 39, the tetragonal phase in Refs. 40–43, and the rhombohedral phase in Ref. 44). Under ultrahigh P and T, 3D polymers have been discovered, but, as yet, without a uniform structure.

A. Bonding in HPHT polymeric C_{60}

C_{60}, an electron-deficient polyene, tends to react with other molecules via radical, nucleophilic, or cycloaddition

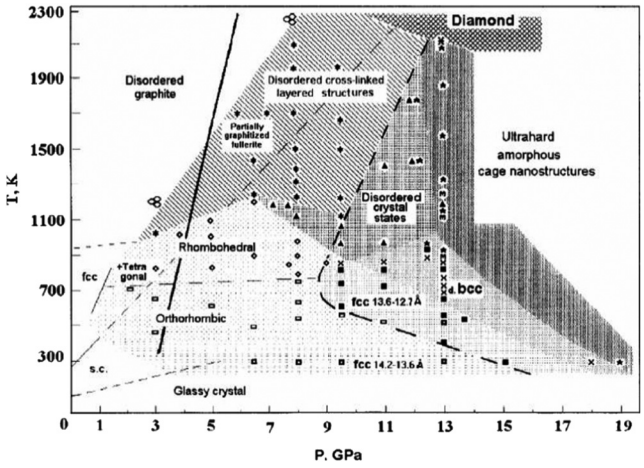

FIG. 1. Map of the P–T plane showing the various phases of C_{60} created under different conditions. Symbols denote some of the P–T coordinates where experiments have been carried out and samples have been treated for at least 1 min. (—) denotes the diamond/graphite equilibrium line, while (– – –) divides the semimetal and semiconductor states at $T > 1100$ K and the "soft" and "hard" states at $T < 1100$ K. Reprinted with permission from V. D. Blank *et al.*, Carbon **36**, 319–343 (1998). Copyright 1998 Elsevier.

mechanisms. Fullerene can be functionalized via [2 + n] cycloaddition (n = 1, 2, 3, 4) reactions.[45] In P-induced polymerization, a [2 + 2] cycloaddition reaction between two [6,6] double bonds of near-neighbor C_{60} cages is the favored reaction pathway (Fig. 2). A new cyclobutane ring is formed by covalent linkage in the polymeric product. On the other hand, the formation of C_{60} intermolecular bonds is a thermally activated process, and the polymerization reaction is very slow at room temperature. Davydov *et al.*[46] have shown that the activation energy for the formation of the C_{60} dimer is approximately 135 kJ mol^{-1}. However, at ambient P and T between 300 °C and 400 °C, the polymeric product is metastable and reverts to pristine C_{60}.[32] Hence, P is necessary for the formation of a stable polymeric product because it reduces the intermolecular distance sufficiently for chemical bond formation to take place.

In the 3D C_{60} polymer, [3 + 3] cycloaddition bonds form between 2D layers to construct a 3D framework, and it is a fragment of the di-(1.5)(6,10)methanol-cyclodecane molecule.[47,48] All the equivalent 3 and 6 atoms of each C_{60} molecule are bonded in pairs with the corresponding atoms of the neighboring (x,y) layer molecules. The intermolecular bond lengths are 0.151 nm and 0.161 nm for the [3 + 3] and [2 + 2] cycles, respectively.[47]

The distance between the center-of-mass positions of the two nearest-neighbor C_{60} in face-centered cubic (fcc) bulk C_{60} is 10.1 Å.[49] Generally, it is 9.1 Å in C_{60} [2 + 2] cycloaddition polymers and about 9.4 Å when a single C–C bond links two cages.[50,51] For example, the intermolecular distance along the C_{60} orthorhombic chains is 9.14 Å, as characterized by single-crystal X-ray diffraction experiments.[39] In confined C_{60}, the nearest-neighbor cage distance approaches a value of 8.45 Å near 10 GPa.[52]

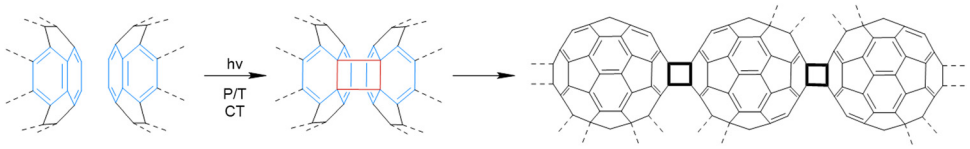

FIG. 2. Formation of C_{60} polymers by [2 + 2] cycloaddition of pristine C_{60}. (The figure has been redrawn based on Ref. 26.) Reprinted with permission from F. Giacalone and N. Martín, Chem. Rev. **106**, 5136–5190 (2006). Copyright 2006 American Chemical Society.

Alkali-metal-doped fullerene polymerizes under high T or HPHT. However, the framework is constructed using single carbon bonds.[53] In the case of endohedral fullerenes with C_{80}, [2 + 2] cycloaddition reactions occur at both the [6,6] and [5,6] bonds of the cage. The [6,6]-regioisomer is a kinetic product, while the [5,6]-regioisomer is a thermodynamic product.[54]

B. Spectroscopy of monomeric, dimeric, and polymeric phases

Polymerization changes both the microscopic and macroscopic properties of a material. Insolubility of the polymeric materials in those solvents that do dissolve C_{60} is direct proof of the polymerization. Polymerization is also confirmed by shifts in the vibrational modes and activation of Raman and infrared modes due to the reduced molecular symmetry as well as to the greater degree of freedom, and these also indicate the degree of polymerization (Fig. 3). According to the symmetry of the displacement patterns, there are 46 distinct intramolecular vibrations for C_{60}. Group theory indicates ten first-order Raman-active modes, including two breathing A_g modes related to the symmetric oscillations of the entire molecule and pentagons together with eight H_g modes.[55–60] In addition, four intramolecular T_{1u} modes are infrared-active at first order.[55,61,62] The Raman (Fig. 3) and infrared (IR) spectra of the

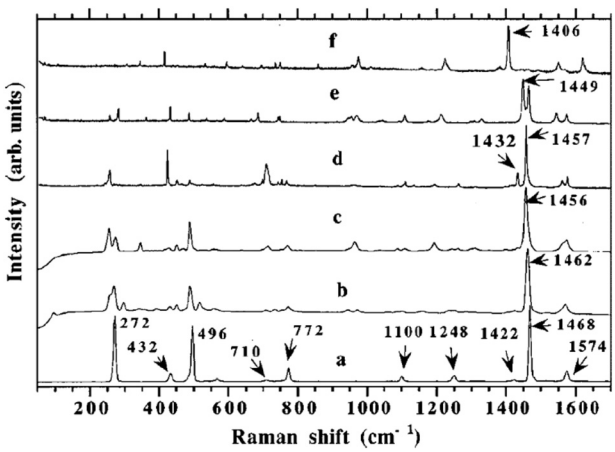

FIG. 3. Raman spectra of pristine C_{60} (a), polymerized dimers (b), and orthorhombic phase (c), excited by a 1064 nm line, and of the orthorhombic (d), tetragonal (e), and rhombohedral (f) phases, excited by a 568.2 nm line. Reprinted with permission from V. A. Davydov *et al.*, Phys. Rev. B **61**, 11936 (2000). Copyright 2000 American Physical Society.

pressure-dimerized state, as well as those of the orthorhombic, tetragonal, and rhombohedral pressure-polymerized phases of C_{60}, have been investigated.[55]

The number of covalent bonds per C_{60} molecule increases with increasing P and T. Accordingly, the formation of intermolecular bonds shifts the electron density away from the remaining double bonds, which become weaker. In particular, the $A_g(2)$ mode is one of the most sensitive to polymer structure and charge transfer. As shown in Fig. 3, it downshifts from 1470 cm^{-1} in the monomer to 1465 cm^{-1} in the dimer, which corresponds to two sp^3-like coordinated carbon atoms per fullerene molecule.[63] Upon further polymerization, the softening is 12 cm^{-1} in the linear polymeric chains, 20 cm^{-1} in the planar tetragonal phase, and 60 cm^{-1} in the 2D rhombohedral polymers.[55] Apart from this, the presence of sp^3 intermolecular bonds leads to the appearance of new bonds in the range 900–1000 cm^{-1}.

Thermally induced dissociation of the polymeric bonds in C_{60} polymers can be monitored as a function of time at high T. For example, the band shape and the intensity of the $A_g(2)$ mode change with increasing time.[64] Novel polymeric C_{60} phases can also be recognized by Raman spectroscopy measurements. For instance, a branched-chain C_{60} polymer shows a characteristic mode at 1454 cm^{-1}, a more pronounced splitting of $H_g(1)$, and a new Raman-activated mode around $A_g(1)$.[63]

The symmetry of C_{60} is reduced from I_h to D_{2h} in the orthorhombic and tetrahedral polymers and to D_{3d} in the rhombohedral phase.[65] Accordingly, the $T_{1u}(2)$ mode is primarily polarized in the stretched directions and dramatically downshifts more than 50 cm^{-1} in the IR spectra of the orthorhombic and rhombohedral polymers. The large distortions of the C_{60} sphere due to the numbers of cycloaddition connections demand a distorted polymer C_{60} ball with relaxed atomic positions.

C. Dimerization of C_{60} at HPHT

Before discussing the formation and structures of polymeric C_{60}, we briefly review the structural features of C_{60} at ambient P. C_{60} molecules exhibit a rotationally disordered fcc structure above 260 K, free rotation at high T, and an orientationally disordered phase at 90 K. Under compression, the crystal undergoes an orientational transition at around 0.4 GPa and ambient T, which transforms into a simple cubic (sc) structure.[2,13,66] During further shortening of the intermolecular distance, [6,6] double bonds open and four-membered rings link nearest neighbor cages. A solid-state mechanochemical method shows that the C4 ring connecting the cages is square rather than rectangular. As shown in Fig. 4, C_{60} dimers are disordered in position and orientation within an average cubic lattice derived

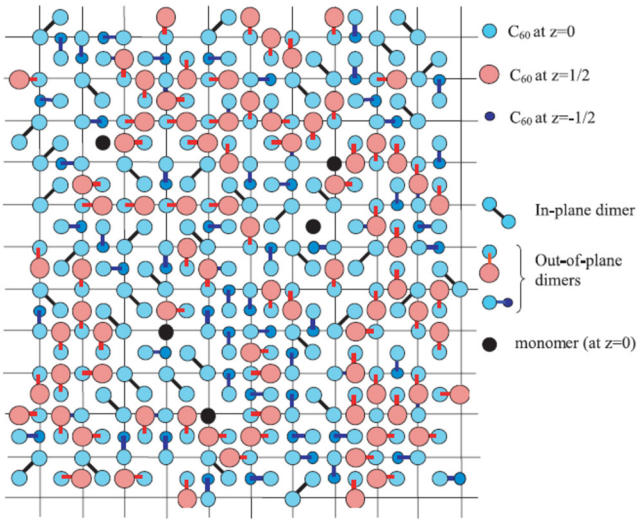

FIG. 4. A random distribution of C_{60} dimers (and isolated monomers) in the (001) plane of a model crystal, which accounts reasonably well for the experimentally observed diffuse scattering intensity distribution. Only in-plane and out-of-plane C_{60}'s that form dimers with an in-plane C_{60} are shown. Reprinted with permission from R. Moret *et al.*, Eur. Phys. J. B **37**, 25–37 (2004). Copyright 2004 Springer Nature.

from the monomer.[67] C_{60} dimerization begins either within the fcc phase, in which the cage rotates freely, or within the sc structure with nearest neighbors in the P-DB (C=C double bond facing pentagon) or H-DB (C=C double bond facing hexagon) configuration.[68] This mechanism can be observed even at room temperature at about 1.0 GPa.[69] However, this thermally activated process is very slow at ambient T. As a result, direct synthesis of pure C_{60} dimers at HPHT is not yet possible. Typical conditions for synthesizing the C_{60} dimer are 1.5 GPa, 423 K, and 1000 s, with a yield of about 80%.[55] When the C_{60} molecules are linked, the icosahedral symmetry is drastically reduced. As a consequence, the degenerate energy levels near the Fermi level are removed, and thus the optical band gap narrows.[70]

D. 1D polymerization of C_{60} at HPHT

At higher T (<700 K) and P (~0.7–9 GPa), long linear chains with two four-membered rings per C_{60} cage form. Parallel straight chains along the original ⟨110⟩ directions in the ordered orthorhombic structure are observed in powder and single-crystal diffraction results, although disordered branched chains possibly exist as well (Fig. 5). At the same time, a large and rapid change in volume at P ~ 1 GPa has been observed.[71] The XRD pattern confirms that the nearest-neighbor distance (about 9.1–9.2 Å) in the orthorhombic phase polymer decreases by almost 10% compared with 10.02 Å in pristine C_{60}, owing to the formation of covalent bonds.[39,55] It is interesting to note that two different orthorhombic phase C_{60} polymers can be formed, corresponding to "high" (above ~2–3 GPa) and "low" P regions. These structures are recognized by the different orientations of the chains around their axes. The chain links are parallel to the plane in the orthorhombic (O) structure,[33] while they are alternately tilted by angles $+\mu$ and $-\mu$ from chain to chain in another orthorhombic (O′) phase.[39,72] As a result, the O and O′ phases demonstrate a pseudo-tetragonal *Immm* space group and orthorhombic *Pmnn* space group, respectively. It is hard to estimate the angle μ, but lattice energy minimization predicts an optimal value of 29°.[68]

E. 2D polymerization of C_{60} at HPHT

At higher T (>700 K) and P (1.5–9 GPa), four or six four-membered rings per C_{60} molecule participate in the construction of the 2D C_{60} polymer. The formation of the polymer layers by cross-coupling of chains appears in two possible unit cells (tetragonal and trigonal). After that, the layers stack in a close-packed arrangement to form the corresponding tetragonal or rhombohedral structures. When [2 + 2] cycloaddition occurs in the (001) plane of the original fcc phase, a 2D tetragonal phase is formed [shown in Fig. 3(e)].[2] For example, a single crystal of the "tetragonal" polymer was obtained when C_{60} was treated at 2.5 GPa and 500 °C.[43] A single-crystal study identified the tetragonal phase to be a pseudo-tetragonal

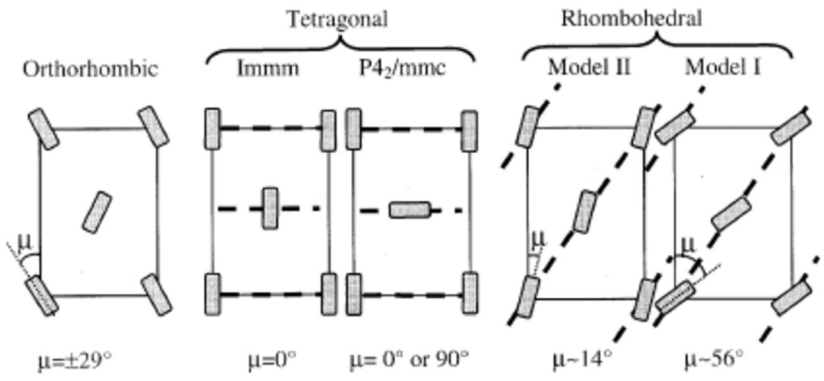

FIG. 5. Schematic views of the polymer chains running along ⟨110⟩ cubic directions of the parent monomer lattice, for the different polymer structures. The chains are normal to the figure. The orientation of the four-membered rings is represented by the shaded bars that form an angle μ with the ⟨001⟩ cubic directions. The broken lines represent the 2D tetragonal and rhombohedral polymer layers that can be obtained, at least schematically, by connecting the C_{60} molecules of the chains by supplementary four-membered rings. Reprinted with permission from R. Moret *et al.*, AIP Conf. Proc. **544**, 81–84 (2000). Copyright 2000 AIP Publishing LLC.

packing of translationally identical adjacent 2D layers with an orthorhombic space group *Immm*.[43] In this case, the chain orientations are almost parallel. In another case, the chain links are alternately parallel and perpendicular to the stacking axis and exhibit a $P4_2/mmc$ space group. Interestingly, Wågberg *et al.*[74] reported that the structural transition from an orthorhombic to a tetragonal structure occurs via an intermediate dimer state as an orthorhombic phase to a dimer and then from this dimer to a tetragonal phase. In addition, the second process is slower than the first.

When treated at higher P (500–800 °C at 5 GPa), C_{60} polymerized via [2 + 2] cycloaddition in the (111) plane of the original fcc phase into a rhombohedral structure with a hexagonal lattice.[2,32] It has been reported that during decompression from 6 GPa to 2.2 GPa at 873 K, the rhombohedral polymer could transform to a tetragonal phase.[40] A trigonal symmetry instead of a hexagonal one was confirmed to be the most stable mode by an XRD experiment.[75] The hexagonal layers stack in a close-packed arrangement of the ABCABC type with space group *R*3-*m*.[33,76] All the former four-membered rings rotate 60°, forming another structure with ACBACB stacking type. Single-crystal XRD studies confirm this structure,[42] and a density functional theory (DFT) calculation demonstrates slightly more stability.[77]

F. 3D polymerization of C_{60} at HPHT

Under much higher P (>13 GPa) at elevated T, 3D polymers are obtained. For example, one superhard phase of a 3D polymer quenched from 13 GPa and 820 K features [3 + 3] cycloaddition bonding between the [2 + 2] cycloaddition-bonded 2D tetragonal layers.[47,48] Single-crystal XRD results demonstrate that the 3D C_{60} polymer is in a body-centered orthorhombic space group *Immm* structure (Fig. 6).[78] The resulting sp^3–sp^2 hybridized system is expected to show metallic conductivity. In contrast, the 2D rhombohedral phase transforms into a disordered phase at around 15 GPa,[79] and the 2D tetragonal phase transforms into a 3D metastable polymer over 20 GPa at room temperature.[80] *In situ* Raman spectra strongly support the above conclusion by revealing a transformation from a 2D to a 3D phase.[81–84] Also, the *in situ* X-ray measurements reveal a first-order irreversible transition of the tetragonal polymeric phase at around 24 GPa.[82]

Although several studies have demonstrated the existence of 3D C_{60} polymers, there is still no consensus on the preparation conditions, owing to experimental difficulties and the structural complexity of the products. Generally, under 8–9 GPa, a cubic structure is observed up to about 600–700 K. Disorder increases, and covalent linking extends in all directions with rising T.[5,68] Over 9.5 GPa, a body-centered structure presents.[78] When T rises above 900–1000 K, the C_{60} cages start to collapse, and this, combined with the covalent bonding distortion of the cage, makes the structure become amorphous or even graphitic at higher T.[4] Superhard materials, even cubic diamond crystallites, have also been found.[85]

In conclusion, several tentative phase diagrams of C_{60} at HPHT have been reported.[2,4,55,76] It should be noted that the polymeric phase formation and purity depend strongly on T, P, and treatment time. Typical conditions for the formation of C_{60} polymers are as follows: for the 1D orthorhombic phase, 1–1.2 GPa, 550–585 K for 5 h;[39,55] for the 2D tetragonal phase, 2–2.5 GPa, 700–873 K for 0.5–4 h;[42,43,55] and for the 2D rhombohedral phase, 5–6 GPa, 773–873 K for 0.5–1 h.[44,55] Another problem is establishing the stability of the polymeric phases. A quenched intermediate transition or experimental artifacts all possibly exist, but only a few *in situ* studies have been carried out.

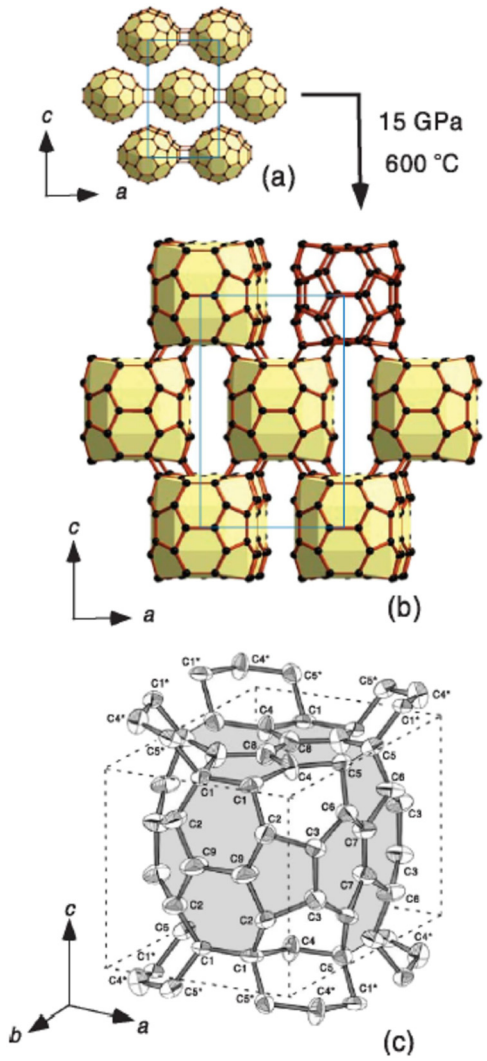

FIG. 6. Crystal structure of the 3D C_{60} polymer (b) in comparison with the starting 2D polymer (a). Carbon atoms marked with * in (c) are from the neighboring C_{60} units. Reprinted with permission from S. Yamanaka *et al.*, Phys. Rev. Lett. **96**, 076602 (2006). Copyright 2006 American Physical Society.

It is important to highlight that heating-then-pressing from rapidly rotating monomers leads to disordered states, because chains form in all directions. Compression benefits the formation of well-ordered 1D or 2D polymers. Nevertheless, pressing-then-heating favors the optimal [2 + 2] cycloaddition route to dimerization, but orientational tuning at high T

promotes linear or planar bonding.[68] However, different paths still give distinct products. For instance, the heating-then-pressing path tends to form rhombohedral polymers.[82]

When we consider the polymeric phase transition shown in Fig. 1, the orthorhombic-to-tetragonal transformation involves proper rotations of the chains followed by interchain cross-linking in the $\{100\}_c$ planes. Furthermore, the transformation from an orthorhombic to a rhombohedral phase demands that the chains rotate to a fixed angle, while the tetragonal-to-rhombohedral transition requires bond rearrangement (Fig. 5).[73]

G. Properties of polymeric C_{60} phases

The physical properties of the low-dimensional phases have already been well studied.[2,4] The essential difference between the C_{60} monomer and the polymers is the covalent intermolecular linkage in the latter. ^{13}C nuclear magnetic resonance (NMR) studies of orthorhombic,[86,87] tetragonal,[88] and rhombohedral[86,89] C_{60} clearly demonstrate that these structural differences are based on the distinguishable frequencies of sp^2 and sp^3 hybridized carbon. The relative numbers of sp^2 and sp^3 hybridized atoms can be used to identify the intra- and intermolecular bonds in the polymeric phase. In particular, the sp^2 peak can be decomposed into lines corresponding to the number of unique carbon atom environments (Fig. 7).[88,89]

The reduced symmetry of icosahedral C_{60} and the formation of intermolecular bonds in the polymeric phase lead to splitting of degenerate molecular orbitals and a narrowing of the HOMO–LUMO gap. The electronic structures of 1D and 2D C_{60} polymers have been studied theoretically. The 1D linear polymer is a semiconductor with a finite band gap of 1.148 eV and almost pure s-type intermolecular bonding.[90] The 2D tetragonal and rhombohedral C_{60} polymers are also semiconductors. With different intermolecular covalent bonds, the tetragonal polymeric and rhombohedral polymeric phases exhibit band gap values of 1.2 eV and 1.0 eV, respectively.[34]

C_{60} is reportedly stable up to 950 °C under low-pressure inert gas conditions.[91] High-temperature synchrotron radiation XRD results show that C_{60} is stable below temperatures of 900 °C at 80 MPa.[92] However, all the polymers are less stable than the monomer with free C_{60} molecules. For example, dimers are stable to about 420 K,[93,94] the orthorhombic phase breaks down near 500 K, and the tetragonal and rhombohedral 2D polymers are stable to 550 K.[94,95] Thus, the stability sequence is dimer < 1D polymer < 2D polymer < monomer.[34] It should be noted that the thermal "stability limit" is dependent on time scale. The activation energy E_a reflects the stability of the polymers; it is 1.75 eV and 1.9 eV for the dimers and orthorhombic C_{60} polymeric phases, respectively.[34,94]

The degree of polymerization, the polymeric structure, and the ratio of sp^2 to sp^3 C dominate the conductivity of polymerized C_{60}. In contrast to C_{60}, an n-type semiconductor, the 1D plasma-polymerized C_{60} polymer acts as a p-type semiconductor in field effect transistor (FET) experiments owing to variable-range hopping (VRH).[96] With the increasing degree of polymerization, the band gap reduces and the electrical conductivity increases.[95] The conductivity of 2D C_{60} polymers is anisotropic. In the covalent bond linking layer, it shows a metallic-like behavior. In the weak van der Waals interacting direction of the interlayers, it exhibits semiconductor-like behavior.[97,98] This phenomenon is ascribed to the weak localization of the carriers, and the metallic behavior could be attributed to a self-doping effect. Structural calculations show that lattice defects may induce metallic behavior.[99] Electrical resistivity measurements show that amorphous polymeric C_{60} phases are semimetallic, with VRH and semiconducting behavior.[100] Recent first-principles DFT calculations have demonstrated that the structures of 3D C_{60} polymers in which each molecule is in one of the two standard orientations are analogous to ordered binary-alloy-type structures.[101] Furthermore, all the investigated structures in this case are predicted to be metallic, which is supported by an experimental result where a polymeric 56/56 2 + 2 cycloaddition bond is analogous to the Ising antiferromagnetic interaction in a 3D C_{60} polymer.[102]

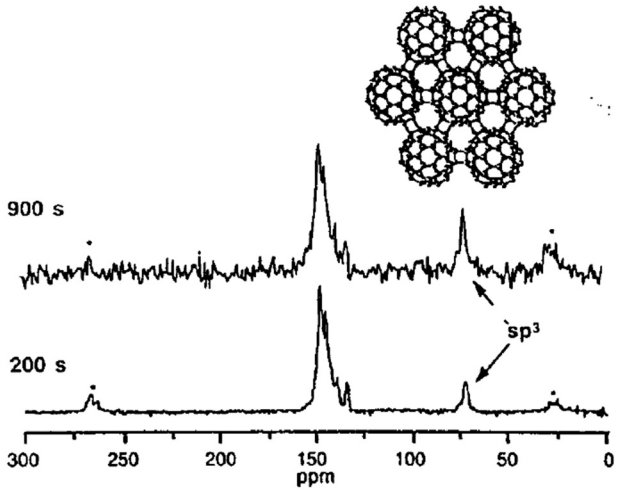

FIG. 7. ^{13}C magic angle spinning (MAS) NMR spectra of the rhombohedral 2D phase with a spinning rate of 12 kHz and repetition times of 200 and 900 s. The inset shows the structural mode of this phase. Reprinted with permission from F. Rachdi *et al.*, J. Phys. Chem. Solids **58**, 1645–1647 (1997). Copyright 1997 Elsevier.

Thermal conductivity theoretically increases with increasing P. In addition, it increases with the formation of covalent bonds between near neighboring C_{60}'s because the resulting appearance of new phonon modes contributes to heat transport. Polymeric phase disorder will compensate for the thermal conductivity effect.[103]

III. HPHT RESEARCH ON C_{70}

C_{70} molecules undergo quasi-free rotation in a close-packed fcc lattice above room temperature. However, only the five bonds radiating out from each polar pentagon have significant reactivity, which leads to topological constraints on the formation of C_{70} polymers. The anisotropic C_{70} molecule exhibits at least three phases: free rotation at high T, uniaxial rotation at intermediate T, and frozen rotation or ratcheting at low T.[3,104]

Under compression, the rotational motion is reduced to uniaxial rotation around the molecular axis. Subsequently, the C_{70} molecules tend to arrange in a line, and a rhombohedral structure is obtained (Fig. 8).[106,107] Regarding symmetry, the C_{70} monomer with an fcc lattice cannot form a long-range ordered polymeric structure. In contrast, C_{70} crystallized in the hcp structure can polymerize into an ordered zig-zag chain structure with an orthorhombic lattice.[108]

At T between 400 and 500 K and P around 1 GPa, a dimer-rich phase is observed, while the dimer ratio reduces at higher temperatures. Notably, C_{70} exhibits lower reactivity than C_{60},[105] so the dimerization of C_{70} is much slower under high P.

Several polymeric phases have been observed in C_{70} at higher P and T. Incompatibility between the lattice symmetry and the geometry of the reactive bonds means that an ordered polymeric phase of C_{70} is hard to obtain at P in the range of 0.82 GPa at T between 350 and 600 K. However, Blank *et al.*[109,110] and Marques *et al.*[111,112] reported that C_{70} with an fcc lattice could transform to an ordered structure under sufficiently high P, which was thought to occur only in hcp C_{70}. It should be noted that the low reactivity and topochemical constraints on the polymerization lead to the slower formation of C_{70} oligomers and polymers. Above 700 K, a "disordered cross-linked layered" structure and a 3D polymerized tetragonal structure have been reported.[109]

IV. HPHT RESEARCH ON INTERCALATED FULLERENE

A. Solvent effect on parent structure at ambient conditions

The interaction between fullerenes and solvents leads to the formation of solvated fullerene.[113] C_{60} and C_{70} can form solvated crystals with almost all common solvents.[12]

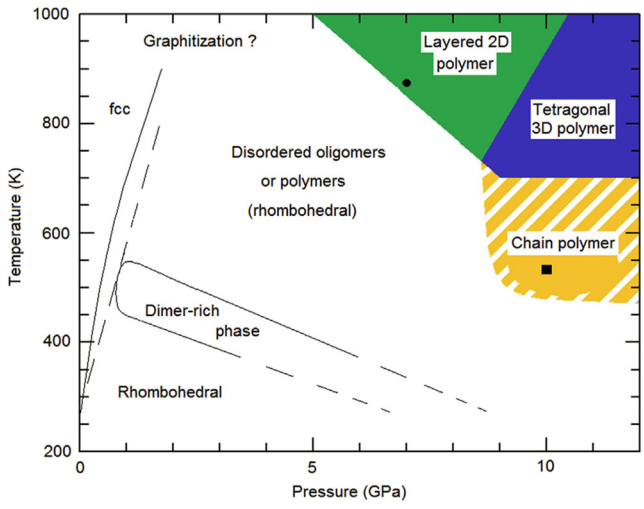

FIG. 8. Structural phase diagram of C_{70} with an fcc structure under ambient conditions. Reprinted with permission from B. Sundqvist, Carbon **125**, 258–268 (2017). Copyright 2017 LW Elsevier.

Evaporating fullerene solutions is the general preparation method to obtain solvated fullerenes. In 1991, Fleming *et al.*[114] reported solvated C_{60} and C_{70} for the first time, inspiring subsequent research on the synthesis and characterization of this series of materials.[115–122] Several conclusions have been drawn based on this research:

(a) Solvates are typical van der Waals complexes with negative excess volumes. Bonding between fullerenes and a solvent will enhance the stability of the solvate.[120]
(b) Synthesis T plays an important role in the stability and stoichiometry of solvated fullerenes.[14,15,120,123]
(c) Incorporated solvent molecules influence the crystal structure. There are at least five types of packing symmetry (hexagonal in C_{60}*2$BrCCl_3$,[116] cubic in C_{60}*cyclohexane,[118] monoclinic in C_{60}*$C_6H_5CH_3$,[123,124] triclinic in C_{60}*2ferrocene,[122] and orthorhombic in C_{60}*1,1,2-trichloroethane[115,125]) in solvated fullerenes. An interesting case is a static cubane, which occupies the octahedral voids of the fcc structures and forms C_{60}*C_8H_8 and maintains the fcc structure (Fig. 9).[49] Accordingly, solvents with symmetrical geometry and a small size tend to occupy the octahedral voids of fullerene lattices and maintain their initial structure, while solvents with non-symmetric geometry or polar molecules are ideal structure controllers.[12,120,123,124,126] Besides the solvent species, the stoichiometric ratio of solvent to C_{60} will also have an impact on the structure of the solvated crystals.[116]

Furthermore, the solvent molecule also affects the physical properties. Świetlik *et al.*[123] and Graja and Świetlik[127] reported that the rotation of C_{60} is hindered by the intercalated solvent molecule, which is reflected in the vibrational spectrum. The influence on the rotation of C_{60} depends dramatically on the intermolecular interaction and structural arrangement. On the other hand, the symmetry decrease due to interactions between fullerene and solvent molecules enhances the photoluminescent intensity. For instance, the intensity rises about two orders of magnitude in C_{60}*m-xylene compared with pristine C_{60} crystal,[12,14] and it is about 30 times higher in C_{70}*mesitylene than in pristine C_{70} powder.[128] The solvent effect on the photoluminescent behavior correlates with the interaction of the cages.[129]

B. Solvent effect under HPHT

Under high P, the incorporated solvent molecule diversified the phase transformation and polymerization of C_{60}. There are four kinds of P-induced solvent effect:

(a) Through a spacer, such as C_8H_8 in the C_{60}*C_8H_8 crystal, which effectively shields the P in the interball voids, raising the phase transition P compared with that of C_{60}.[130]
(b) Through a structure confiner, for instance, 1,1,2-trichloroethane (TCAN), which confines the [2 + 2] cycloaddition bonds of the C_{60}'s that form in the upper and lower layers alternately when C_{60}*1TCAN is treated under high P and high T. As a result, a novel quasi-3D C_{60} polymer is obtained.[17] Another example is C_{60}*m-xylene.[16,131] The

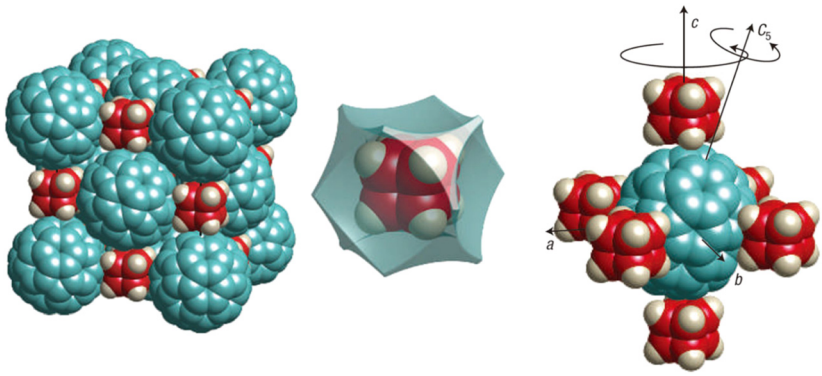

FIG. 9. Structures of fullerene–cubane heteromolecular crystals. (a) Space-filling view of the rotor–stator phase of C_{60}*C_8H_8. Rotating fullerenes occupy the fcc lattice sites, and static cubanes are in between the octahedral voids. (b) The position of cubane in an octahedral void of the fcc cell. The concave outer faces show the perfect match between the cubane and the surrounding fullerenes. (c) The restricted motion of C_{70} in the tetragonal rotor–stator phase of C_{70}*C_8H_8. In the molecular bearing of six cubanes, C_{70} rotates about its long axis (C_5), which processes about the *c* axis of the body-centered tetragonal cell. Reprinted with permission from S. Pekker *et al.*, Nat. Mater. 4, 764–767 (2005). Copyright 2005 Springer Nature.

long-range hcp structure is maintained by the *m*-xylene confiner even when the C_{60} cages collapse at $P > 32$ GPa.

(c) Through a bridge, such as in C_{70}*m-xylene, where the *m*-xylene forms a superhard sp^3-bonded carbon by bonding with neighboring fullerenes.[83]

(d) Through a charge reservoir. For example, the formation of a donor–acceptor complex can be monitored by Raman spectroscopy when C_{60}{Ni(nPr_2dtc)$_2$}, C_{60}{Cu(nPr_2dtc)$_2$}, and C_{60}{Pt(dbdtc)$_2$} are compressed at $P > 0.7$ GPa, 0.7 GPa, and 0.5 GPa, respectively.[132,133] In the case of iodine-doped C_{60}, which crystallizes in a base-centered orthorhombic structure,[134] *P* enhances the charge transfer between the C_{60} and the iodine atoms. As a result, the electrical band gap is 0.3 eV at 17 GPa.

It must also be mentioned that any given solvent molecule generally plays more than one role in the structure control and property tuning of solvated fullerene. For instance, ferrocene acts as a spacer as well as a charge reservoir to tune the polymerization process and promotes a layered structure of the intercalated ferrocene in the $C_{70}(Fe(C_5H_5)_2)_2$ crystal.[135] The *m*-xylene in a C_{60} solvate plays an important role as a spacer and a bridge by forming covalent bonds with neighbors. It preserves the stability of the highly deformed or amorphous C_{60} molecules to form a long-range ordered structure under high *P*.[83] Hence, the solvent effects on the structure and properties of solvated molecules are various and diverse under high *P*.

The *P*-induced polymeric products can be divided into two categories: copolymerized products of C_{60} and solvent molecules, or C_{60} self-condensed materials. C_{60}*C_8H_8 and $C_{60}S_{16}$ are in the former category. An anomaly at 0.5 GPa in the *P* dependences of the molecular vibrational frequencies indicates an orientational ordering transition at room temperature, while an anomaly at 1.3 GPa is attributed to a fullerene–cubane interaction in C_{60}*C_8H_8.[136] In $C_{60}S_{16}$, the peaks from the S_8 rings disappear, and new peaks are observed above 7.2 GPa, suggesting that the sulfur rings break and covalent C–S bonds form between the C_{60} and solvent molecules.[137] In the second category, the C_{60} solvates grown from different solvent molecules exhibit various polymeric products under high *P*. For instance, C_{60}*TDAE [where TDAE is tetrakis(dimethylamino) ethylene] (Refs. 138 and 139) and $C_{60}(Fe(C_5H_5)_2)_2$ (Refs. 140 and 141) both exhibit a one-dimensional polymerized phase above ~1 GPa and 5 GPa, respectively. C_{60}{Pt(dbdtc)$_2$} starts to form intercage covalent bonds at 0.5 GPa and a novel polymer, which is coordinated with nearest-neighbor C_{60} with 10 and 6 sp^3-like carbon atoms per molecule above 2.5 GPa.[132] The solvent molecule in C_{60}*m-xylene confines the formation of ordered amorphous carbon clusters (OACCs) under high *P*, as shown in Fig. 10.[16] This study on a small piece of C_{60} solvate indicates the diversity of the structure and properties of these solvates under high P, and additionally predicts potential applications in a wide range of areas.

Recently, a new way to understand the pressure-induced structure formation and transformation in fullerene solvates under high *P* has been proposed by studies in which their building blocks have been tailored and their boundary interactions have been tuned.[83,84,142,143] Solvent molecules with hexagonal carbon rings, such as *m*-xylene, 1,2,4-trimethylbenzene (TMB), and *m*-dichlorobenzene (m-Cl), tend to stabilize highly compressed or collapsed fullerene clusters in fullerene solvates and form a long-range ordered structure under compression. In contrast, ferrocene, with its pentagonal carbon ring, generally causes a transformation into an amorphous component together with a carbon cage and leads to the formation of a disordered fullerene solvate structure under high *P*. Cubane, C_8H_8, differs from these aromatic solvents. It reacts with C_{60} in solvates under high *P*, but not all of the C_8H_8 molecules react with the carbon cage.[142] The intercalated C_8H_8 and the reacted C_8H_8 both protect the C_{60} cages from early collapse under compression. Furthermore, unlike C_{60}*m-xylene, in which the C_{60} molecules overcome the confining effect of the solvent molecules and take part in polymerization between the cages,[16,84] the absence of intermolecular bonds

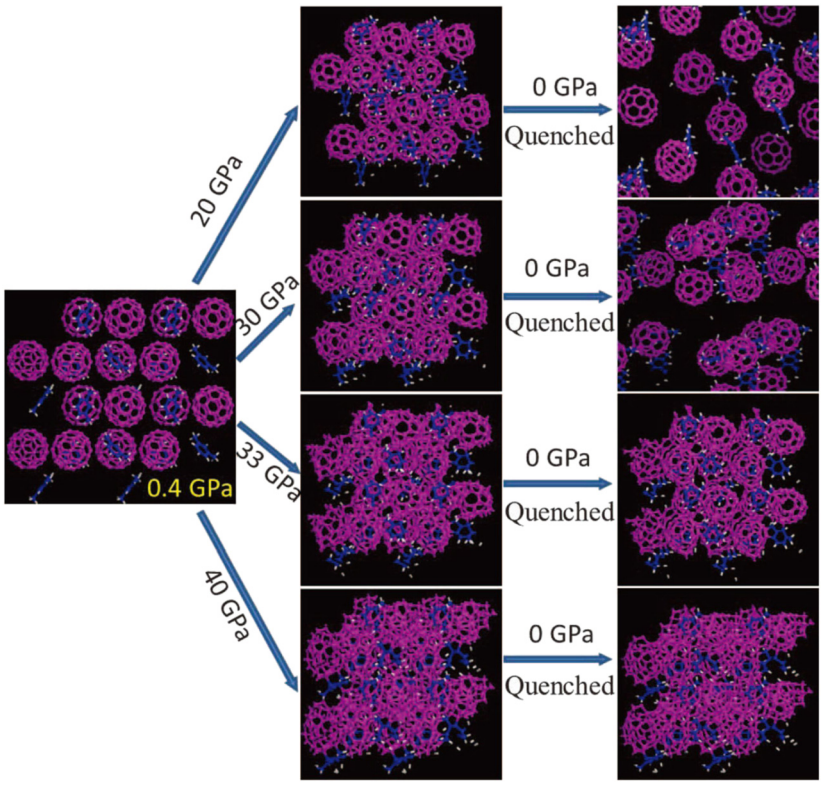

FIG. 10. Simulated structures of C_{60}*m-xylene under different compression and decompression conditions. Far left, the pristine structure at 0.4 GPa. The deformation of the C_{60} cages is elastic below about 30 GPa, and the deformed cages return to their initial shape as they are decompressed back to ambient P. Above 30 GPa, many carbon–carbon bonds start to break, and the cages can no longer return to C_{60} upon decompression. OACCs retain long-range periodicity and can be preserved under ambient P conditions. Reprinted with permission from L. Wang *et al.*, Science **337**, 825–828 (2012). Copyright 2012 The American Association for the Advancement of Science.

between the C_{60} molecules in C_8H_8/C_{60} tunes the boundary interactions of the carbon clusters to retain an ordered arrangement up to 45 GPa.

C. HPHT studies on CNT-confined fullerenes

Confinement of fullerene molecules by the intrinsic structure of a carbon nanotube (CNT) in HPHT synthesis is an important strategy for the polymerization of fullerenes.[144–150] C_{60}'s packed inside single-walled CNTs are considered "peapods"[145] and provide an opportunity to study original quasi-1D fullerene phases. Using high-resolution transmission electron microscopy, Smith and co-workers[145,146] discovered self-assembling C_{60} fullerene chains inside CNTs. Molecular dynamics studies suggest that (9,9) and (10,10) nanotubes with diameter larger than 6.27 Å give the best fit for C_{60}.[147,148] The intercage distance in a CNT was reduced to 8.7 Å under compression to 25 GPa, and a one-dimensional polymer chain was obtained.[20,52] Larger CNTs have more space for the dimensional polymerization of C_{60}, as proven by the observed zigzag structure in C_{60}@CNT(15,15).

In contrast, the anisotropy of C_{70} is reflected by two distinct orientations with regard to the nanotube axis. The C_{70} long axis parallel to the nanotube long axis leads to a lying-down orientation, while perpendicular orientations form when the long axis is rotated 90° to the nanotube axis. The orientation of C_{70} depends on the diameter of the nanotube. C_{60} peapods fully polymerize at 1.5 GPa and 300 °C,[149] while C_{70} peapods do not give a polymeric product even at higher P and T (1.5 GPa and 545 °C, or 2.5 GPa and 300 °C).[104] These results show that CNTs impose much stricter constraints on the reactivity of the ovoid C_{70} than on that of the high-symmetry C_{60}.

Theoretical simulations have predicted several structures of fullerene peapods under high P.[151] In 2017, a novel superhard sp^3 carbon allotrope was obtained by cold compression of C_{70} peapods.[150] This so-called V carbon is thermodynamically stable over a wide P range up to 100 GPa and can be recovered to ambient conditions once it is formed, providing a new strategy for synthesizing new superhard materials.

D. HPHT studies on metal-doped fullerenes

Polymerized alkali-metal-doped fullerenes have attracted much attention because of their hardness and stiffness, metallic behavior,[152,153] and especially superconductivity.[154] 1D and 2D polymeric alkali-metal-doped fullerenes can be obtained under HPHT. For example, AC_{60} (A = K, Rb, Cs) polymerized to a 1D orthorhombic phase under high T.[155] At 5 GPa and 573 K, the 2D

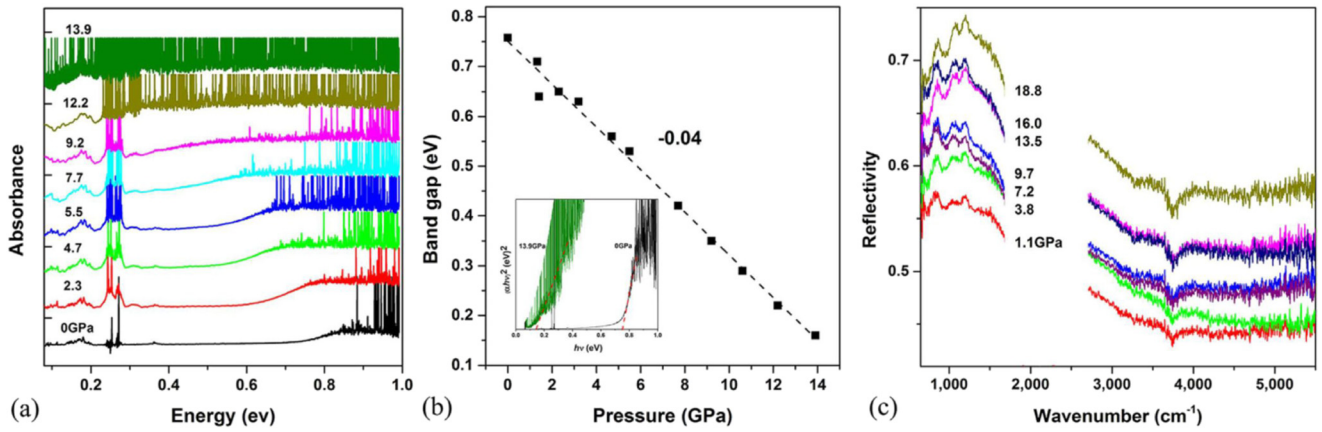

FIG. 11. (a) The mid-IR region shows the absorption edge under high *P*. (b) The band gap as a function of *P*. The inset shows plots of $(\alpha h\nu)^2$ versus $h\nu$ at ambient *P* and at 13.9 GPa. (c) IR reflectivity spectra of the sample under high *P*. Reprinted with permission from J. Cui *et al.*, Sci. Rep. **5**, 13398 (2015). Copyright 2015 Springer Nature.

rhombohedral polymers $(LiC_{60})_{HP}$ and $(NaC_{60})_{HP}$ were synthesized starting from C_{60} and AN_3 (A = Li, Na). Notably, large-radius alkali metals (Rb or Cs) and stoichiometric X_6C_{60} stabilized the doped fullerene at much higher *P* compared with pristine C_{60}. Cs_6C_{60} retains a monomeric structure until 45 GPa,[156] while Rb_6C_{60} exhibits a reversible structural transition to a 2D polymeric phase at 35 GPa and 600 K.[157] A 3D polymeric fulleride can be synthesized by compressing 2D Na_4C_{60}.[21] On the other hand, fullerene will polymerize in a lower *P* range when doped with smaller alkali metals such as Na or Li.[153,154] In addition, an intercalated alkali metal with a small radius could diffuse in the fullerene lattice such as in the case of the superionic conductivity in the Li_4C_{60} polymer,[158,159] Na-ion diffusion in Na_2C_{60} results in the formation of polymeric phases of C_{60}.[160]

V. HPHT RESEARCH ON ENDOHEDRAL FULLERENES

As pointed out at the start of this paper, pressure is a fundamental thermodynamic variable that can dramatically alter the atomic and electronic structure of materials, resulting in concomitant changes in their properties. Determining the evolution of the geometric and electronic structure of endohedral fullerenes under high P is particularly important because this information is necessary for understanding the electronic conduction mechanism, for discoveries of novel electronic properties, and for fabricating novel fulleride-based materials. On the other hand, the relatively low yield restricts the characterization of endohedral metallofullerenes by standard measurement techniques, while our limited understanding of cluster structure and properties is another challenge. However, *in situ* measurements at high P in a diamond anvil cell offer a complete workflow to circumvent these problems effectively.

Cui *et al.*[23,24] have conducted high-*P* structural transformation studies on the mono-atom encapsulated fullerenes $Sm@C_{88}$ and solvated $Sm@C_{90}$. The high-*P* *in situ* IR spectra exhibit both red and blue shifts, indicating an anisotropic deformation of the carbon cage under compression. On the basis of these results, together with those of simulations, Cui *et al.* propose that the cage deforms in the vertical direction, changing from an ellipsoidal to an approximately spherical shape. With further compression, a peanut-like structure appears, before the cage finally collapses under higher P. At the same time, there is a significant *P*-induced reduction in the band gap because of the deformation of the carbon cage and the enhanced intermolecular interaction (Fig. 11). In this compression process, the Sm atom plays a role in restraining the compression of adjacent bonds. The structural evolution of solvated $Sm@C_{90}$ under high *P* is almost the same.[24] The solvent molecule plays a role protecting against cage collapse and postpones *P*-induced changes, contributing to the trapping of the metal atom in an OACC.

Polymeric fullerenes such as polymerized C_{60} and C_{70} exhibit unique properties such as high elastic constants and hardness.[161] An HPHT-induced polymerization study of the endohedral fullerene $La@C_{82}$ revealed different polymeric phases such as dimers and 2D and 3D polymers.[22] X-ray and electron diffraction results showed increasing density and disorder when the sample was treated at 9.5 GPa and 520 K. A fraction of dimer and oligomers mixed with mainly monomeric $La@C_{82}$ retained the hcp structure of the pristine sample. The hcp lattice constant decreased dramatically, and small amounts of body-centered tetragonal phase appeared when T was raised to 720 K.

VI. CONCLUSION

HPHT studies on fullerene and its derivatives have been reviewed. The essential differences among the polymeric phases concern the orientational phenomena that they exhibit and the fullerene cage bonding modes. In view of these, various 1D, 2D, and 3D C_{60} polymeric structures prepared under HPHT have been studied, utilizing FTIR and Raman spectroscopy and XRD. C_{70}, a nonspherical carbon cage with lower symmetry than C_{60}, shares the general features of the latter with regard to polymerization, but its polymeric structures exhibit significantly fewer phases. A deeper understanding of the polymerization processes and phase diagrams of the fullerenes will

help promote the synthesis of new polymeric forms with interesting and useful structural, electrical, magnetic, and photoluminescence properties.

Based on a molecular engineering strategy, solvent molecules, CNTs, and metal atoms could be used to control the arrangement of carbon cages in the lattice. Under HPHT, the intercalated units dominate the evolution of the fullerene configuration, constrain polymerization behavior, and determine the structure and properties of the polymeric product. Further efforts are required so that the phase diagrams of these intercalated/doped fullerenes can be drawn. In addition, studies of intercalated/doped fullerenes at high P and very high T (>1000 °C) present exciting opportunities to discover unique carbon phases and even diamond-like polymeric structures.

Endohedral atoms/clusters greatly enrich the properties of fullerenes, and the resulting fullerene derivatives have properties ranging from semiconducting to metallic. In particular, the tunable electronic spin state inside the fullerene cage makes endohedral fullerenes candidates for use in quantum computing. The application of high P is a potentially useful method to control electronic spin and phonon behavior. However, to date, there have been few high-P studies of fullerenes that have considered this topic. Study of endohedral fullerenes at high P is a very recent field and much remains unexplored. What happens to the interplay of carbon cages and the endohedral species under HPHT conditions? How is charge transferred between the carbon cages and the encaged species when the density increases under compression? What unique properties due to the evolution of molecular and electronic structure will endohedral fullerenes exhibit under high P and indeed high T? The need to answer these questions is a strong motivation for further research in this field.

ACKNOWLEDGMENTS

This work was mainly supported by National Science Associated Funding (NSAF, Grant No. U1530402), the Natural Science Foundation of China (Grant No. 11874076), the Science Challenging Program (Grant No. JCKY2016212A501), and the Postdoctoral Science Foundation (2015M572499).

REFERENCES

[1]H. Mao, X. Chen, Y. Ding, B. Li, and L. Wang, "Solids, liquids, and gases under high pressure," Rev. Mod. Phys. **90**, 015007 (2018).

[2]B. Sundqvist, "Fullerenes under high pressures," Adv. Phys. **48**, 1–134 (1999).

[3]B. Sundqvist, "Polymeric fullerene phases formed under pressure," Struct. Bonding **109**, 85–126 (2004).

[4]V. D. Blank, S. G. Buga, G. A. Dubitsky, N. R. Serebryanaya, P. M. Yu, and B. Sundqvist, "High-pressure polymerized phases of C_{60}," Carbon **36**, 319–343 (1998).

[5]S. M. Bennington, N. Kitamura, M. G. Cain, M. H. Lewis, R. A. Wood, A. K. Fukumi *et al.*, "*In situ* diffraction measurement of the polymerization of C_{60} at high temperatures and pressures," J. Phys.: Condens. Matter **12**, L451–L456 (2000).

[6]T. Horikawa, K. Suito, M. Kobayashi, and A. Onodera, "Time-resolved x-ray diffraction study of C_{60} at high pressure and temperature," Phys. Lett. A **287**, 143–151 (2001).

[7]A. V. Talyzin, L. S. Dubrovinsky, T. Le Bihan, and U. Jansson, "Pressure-induced polymerization of C_{60} at high temperatures: An *in situ* Raman study," Phys. Rev. B **65**, 245413 (2002).

[8]B. Liu, Y. Hou, L. Wang, D. Liu, S. Yu, B. Zou *et al.*, "High pressure and high temperature induced polymeric C_{60} nanocrystal," Diamond Relat. Mater. **17**, 620–623 (2008).

[9]Y. Hou, B. Liu, L. Wang, S. Yu, M. Yao, A. Chen *et al.*, "Comparative study of pressure-induced polymerization in C_{60} nanorods and single crystals," J. Phys.: Condens. Mater. **19**, 425207 (2007).

[10]Y. Hou, B. Liu, L. Wang, S. Yu, M. Yao, A. Chen *et al.*, "Photoluminescence properties of high-pressure-polymerized C_{60} nanorods in the orthorhombic and tetragonal phases," Appl. Phys. Lett. **89**, 181925 (2006).

[11]Y. Hou, B. Liu, H. Ma, L. Wang, Q. Zhao, T. Cui *et al.*, "Pressure-induced polymerization of nano- and submicrometer C_{60} rods into a rhombohedral phase," Chem. Phys. Lett. **423**, 215–219 (2006).

[12]L. Wang, "Solvated fullerenes, a new class of carbon materials suitable for high-pressure studies: A review," J. Phys. Chem. Solids **84**, 85–95 (2015).

[13]L. Wang, B. Liu, D. Liu, M. Yao, S. Yu, Y. Hou *et al.*, "Synthesis and high pressure induced amorphization of C_{60} nanosheets," Appl. Phys. Lett. **91**, 103112 (2007).

[14]L. Wang, B. Liu, S. Yu, M. Yao, D. Liu, Y. Hou *et al.*, "Highly enhanced luminescence from single-crystalline C_{60}•1m-xylene nanorods," Chem. Mater. **18**, 4190–4194 (2006).

[15]L. Wang, B. Liu, D. Liu, M. Yao, Y. Hou, S. Yu *et al.*, "Synthesis of thin, rectangular C_{60} nanorods using m-xylene as a shape controller," Adv. Mater. **18**, 1883–1888 (2006).

[16]L. Wang, B. Liu, H. Li, W. Yang, Y. Ding, S. Sinogeikin *et al.*, "Long-range ordered carbon clusters: A crystalline material with amorphous building blocks," Science **337**, 825–828 (2012).

[17]C. Pei, M. Feng, Z. Yang, M. Yao, Y. Yuan, X. Li *et al.*, "Quasi 3D polymerization in C_{60} bilayers in a fullerene solvate," Carbon **124**, 499–505 (2017).

[18]W. Cui, B. Sundqvist, S. Sun, M. Yao, and B. Liu, "High pressure and high temperature induced polymerization of doped C_{60} materials," Carbon **109**, 269–275 (2016).

[19]W. Cui, M. Yao, D. Liu, Q. Li, R. Liu, B. Zou *et al.*, "Pressure induced metastable polymerization in doped C_{60} materials," Carbon **115**, 740–745 (2017).

[20]M. Chorro, S. Rols, J. Cambedouzou, L. Alvarez, R. Almairac, J.-L. Sauvajol *et al.*, "Structural properties of carbon peapods under extreme conditions studied using *in situ* x-ray diffraction," Phys. Rev. B **74**, 205425 (2006).

[21]M. Yao, V. Pischedda, B. Sundqvist, T. Wågberg, M. Mezouar, R. Debord *et al.*, "Pressure-induced transformation in Na_4C_{60} polymer: X-ray diffraction and Raman scattering experiments," Phys. Rev. B **84**, 144106 (2011).

[22]S. G. Buga, V. D. Blank, B. A. Kulnitskiy, N. R. Serebryanaya, M. Klaeser, G. Liu *et al.*, "Structure and properties of solid La@C_{82} endofullerene polymerized under pressure 9.5 GPa and temperature 520-720 K," Synth. Met. **121**, 1093–1096 (2001).

[23]J. Cui, M. Yao, H. Yang, Z. Liu, F. Ma, Q. Li *et al.*, "Structural deformation of Sm@C_{88} under high pressure," Sci. Rep. **5**, 13398 (2015).

[24]J. Cui, M. Yao, H. Yang, Z. Liu, S. Liu, M. Du *et al.*, "Structural stability and deformation of solvated Sm@C2(45)-C_{90} under high pressure," Sci. Rep. **6**, 31213 (2016).

[25]C. Pei, Z. Yan, Z. Yao, G. Liu, S. Samanta, H. Xiao *et al.*, "Pressure-induced anisotropy deformation of fullerene cages and pyramidalization of planar endohedral clusters" (to be published).

[26]F. Giacalone and N. Martín, "Fullerene polymers: Synthesis and properties," Chem. Rev. **106**, 5136–5190 (2006).

[27]A. M. Rao, P. Zhou, K. Wang, G. T. Hager, J. M. Holden, Y. Wang *et al.*, "Photoinduced polymerization of solid C_{60} films," Science **259**, 955–957 (1993).

[28]A. Hayashi, S. Yamamoto, K. Suzuki, and T. Matsuoka, "The first application of fullerene polymer-like materials, $C_{60}Pd_n$, as gas adsorbents," J. Mater. Chem. **14**, 2633–2637 (2004).

[29]A. M. Rao, P. C. Eklund, J.-L. Hodeau, L. Marques, and M. Núñez-Regueiro, "Infrared and Raman studies of pressure-polymerized C_{60}," Phys. Rev. B **55**, 4766–4773 (1997).

[30]N. Takahashi, H. Dock, N. Matsuzawa, and M. Ata, "Plasma-polymerized C_{60}/C_{70} mixture films: Electric conductivity and structure," J. Appl. Phys. **74**, 5790 (1993).

[31]Y. J. Zou, X. W. Zhang, Y. L. Li, B. Wang, H. Yan, J. Z. Cui *et al.*, "Bonding character of the boron-doped C_{60} films prepared by radio frequency plasma assisted vapor deposition," J. Mater. Sci. **37**, 1043–1047 (2002).

[32]Y. Iwasa, T. Arima, R. M. Fleming, T. Siegrist, O. Zhou, R. C. Haddon *et al.*, "New phases of C_{60} synthesized at high pressure," Science **264**, 5170–5172 (1994).

[33]M. Núñez-Regueiro, L. Marques, J.-L. Hodeau, O. Béthoux, and M. Perroux, "Polymerized fullerite structures," Phys. Rev. Lett. **74**, 278–281 (1995).

[34]C. Xu and G. E. Scuseria, "Theoretical predictions for a two-dimensional rhombohedral phase of solid C_{60}," Phys. Rev. Lett. **74**, 274–277 (1995).

[35]R. Moret, T. Wågberg, and B. Sundqvist, "Influence of the pressure-temperature treatment on the polymerization of C_{60} single crystals at 2 GPa-700 K," Carbon **43**, 709–716 (2005).

[36]B. Sundqvist, U. Edlund, P. Jacobsson, D. Johnels, J. Jun, P. Launois *et al.*, "Structural and physical properties of pressure polymerized C_{60}," Carbon **36**, 657–660 (1998).

[37]I. O. Bashkin, A. N. Izotov, A. P. Moravsky, V. D. Negrii, R. K. Nikolaev, Yu. A. Ossipyan *et al.*, "Photoluminescence of solid C_{60} polymerized under high pressure," Chem. Phys. Lett. **272**, 32–37 (1997).

[38]A. N. Andriotis, M. Menon, R. M. Sheetz, and L. Chernozatonskii, "Magnetic properties of C_{60} polymers," Phys. Rev. Lett. **90**, 026801 (2003).

[39]R. Moret, P. Launois, P.-A. Persson, and B. Sundqvist, "First x-ray diffraction analysis of pressure polymerized C_{60} single crystals," Europhys. Lett. **40**, 55–60 (1997).

[40]V. A. Davydov, L. S. Kashevarova, A. V. Rakhmanina, V. Agafonov, H. Allouchi, R. Céolin *et al.*, "Tetragonal polymerized phase of C_{60}," Phys. Rev. B **58**, 14786–14790 (1998).

[41]V. A. Davydov, V. Agafonov, H. Allouchi, R. Céolin, A. V. Dzyabchenko, and H. Szwarc, "Tetragonal polymerized phase of C_{60}: Experimental artifact or reality?," Synth. Met. **103**, 2415–2416 (1999).

[42]R. Moret, P. Launois, T. Wågberg, and B. Sundqvist, "High-pressure synthesis, structural and Raman studies of a two-dimensional polymer crystal of C_{60}," Eur. Phys. J. B **15**, 253–263 (2000).

[43]X. Chen and S. Yamanaka, "Single-crystal x-ray structural refinement of the 'tetragonal' C_{60} polymer," Chem. Phys. Lett. **360**, 501–508 (2002).

[44]X. Chen, S. Yamanaka, K. Sako, Y. Inoue, and M. Yasukawa, "First single-crystal x-ray structural refinement of the rhombohedral C_{60} polymer," Chem. Phys. Lett. **356**, 291–297 (2002).

[45]M. A. Yurovskaya and I. V. Trushkov, "Cycloaddition to buckminsterfullerene C_{60}: Advancements and future prospects," Russ. Chem. Bull. **51**, 367–443 (2002).

[46]V. A. Davydov, L. S. Kashevarova, A. V. Rakhmanina, V. M. Senyavin, O. P. Pronina, N. Oleinikov *et al.*, "Pressure-induced dimerization kinetics of fullerene C_{60}," J. Exp. Theor. Phys. Lett. **72**, 557–560 (2000).

[47]L. A. Chernozatonskii, N. R. Serebryanaya, and B. N. Mavrin, "The superhard crystalline three-dimensional polymerized C_{60} phase," Chem. Phys. Lett. **316**, 199–204 (2000).

[48]N. R. Serebryanaya and L. A. Chernozatonskii, "Modelling and interpretation of the experimental data on the 3D polymerized C_{60} fullerites," Solid State Commun. **114**, 537–541 (2000).

[49]S. Pekker, É. Kováts, G. Oszlányi, G. Bényei, G. Klupp, G. Bortel *et al.*, "Rotor-stator molecular crystals of fullerenes with cubane," Nat. Mater. **4**, 764–767 (2005).

[50]M. Álvarez-Murga and J. L. Hodeau, "Structural phase transitions of C_{60} under high-pressure and high-temperature," Carbon **82**, 381–407 (2015).

[51]V. A. Davydov, L. S. Kashevarova, A. V. Rakhmanina, A. V. Dzyabchenko, V. N. Agafonov, P. Dubois *et al.*, "Identification of the polymerized orthorhombic phase of C_{60} fullerene," J. Exp. Theor. Phys. Lett. **66**, 120–125 (1997).

[52]S. Kawasaki, T. Hara, T. Yokomae, F. Okino, H. Touhara, H. Kataura *et al.*, "Pressure-polymerization of C_{60} molecules in a carbon nanotube," Chem. Phys. Lett. **418**, 260–263 (2006).

[53]G. Oszlányi, G. Baumgartner, G. Faigel, and L. Forró, "Na_4C_{60}: An alkali intercalated two-dimensional polymer," Phys. Rev. Lett. **78**, 4438–4441 (1997).

[54]N. Chen, E.-Y. Zhang, K. Tan, C. R. Wang, and X. Lu, "Size effect of encaged clusters on the exohedral chemistry of endohedral fullerenes: A case study on the pyrrolidino reaction of $Sc_xGd_{3-x}N@C_{80}$ (x = 0 − 3)," Org. Lett. **9**, 2011–2013 (2007).

[55]V. A. Davydov, L. S. Kashevarova, A. V. Rakhmanina, V. M. Senyavin, R. Céolin, H. Szwarc *et al.*, "Spectroscopic study of pressure-polymerized phases of C_{60}," Phys. Rev. B **61**, 11936 (2000).

[56]Z. Dong, P. Zhou, J. M. Holden, P. C. Eklund, M. S. Dresselhaus, and G. Dresselhaus, "Observation of higher-order Raman modes in C_{60} films," Phys. Rev. B **48**, 2862–2865 (1993).

[57]K. Wang, Y. Wang, P. Zhou, J. M. Holden, S. Ren, G. T. Hager *et al.*, "Raman scattering in C_{60} and alkali-metal-doped C_{60} films," Phys. Rev. B **45**, 1955–1958 (1992).

[58]P. Zhou, K. Wang, Y. Wang, P. C. Eklund, M. S. Dresselhaus, G. Dresselhaus *et al.*, "Raman scattering in C_{60} and alkali-metal-saturated C_{60}," Phys. Rev. B **46**, 2595–2605 (1992).

[59]D. S. Bethune, G. Meijer, W. C. Tang, and H. J. Rosen, "The vibrational Raman spectra of purified solid films of C_{60} and C_{70}," Chem. Phys. Lett. **174**, 219–222 (1990).

[60]S. J. Duclos, R. C. Haddon, S. Glarum, and A. F. Hebard, "Raman studies of alkali-metal doped A_xC_{60} films (A = Na, K, Rb, and Cs; x = 0, 3, and 6)," Science **254**, 1625–1627 (1991).

[61]K.-A. Wang, A. M. Rao, P. C. Eklund, M. S. Dresselhaus, and G. Dresselhaus, "Observation of higher-order infrared modes in solid C_{60} films," Phys. Rev. B **48**, 11375–11380 (1993).

[62]H. Kuzmany, R. Winkler, and T. Pichler, "Infrared spectroscopy of fullerenes," J. Phys.: Condens. Matter **7**, 6601–6624 (1995).

[63]T. Wågberg, P. Jacobsson, and B. Sundqvist, "Comparative Raman study of photopolymerized and pressure-polymerized C_{60} films," Phys. Rev. B **60**, 4535–4538 (1999).

[64]T. Wågberg, P.-A. Persson, B. Sundqvist, and P. Jacobsson, "A Raman study of polymerised C_{60}," Appl. Phys. A **64**, 223–226 (1997).

[65]Z.-T. Zhu, J. L. Musfeldt, K. Kamarás, G. B. Adams, J. B. Page, V. A. Davydov *et al.*, "Far-infrared vibrational properties of tetragonal C_{60} polymer," Phys. Rev. B **65**, 085413 (2002).

[66]L. Pintschovius, O. Blaschko, G. Krexner, and N. Pyka, "Bulk modulus of C_{60} studied by single-crystal neutron diffraction," Phys. Rev. B **59**, 11020–11026 (1999).

[67]R. Moret, P. Launois, T. Wågberg, B. Sundqvist, V. Agafonov, V. A. Davydov *et al.*, "Single-crystal structural study of the pressure-temperature-induced dimerization of C_{60}," Eur. Phys. J. B **37**, 25–37 (2004).

[68]R. Moret, "Structures, phase transitions and orientational properties of the C_{60} monomer and polymers," Acta Crystallogr., Sect. A: Found. Adv. **61**, 62–76 (2005).

[69]V. A. Davydov, L. S. Kashevarova, A. V. Rakhmanina, V. Agafonov, H. Allouchi, R. Céolin *et al.*, "Particularities of C_{60} transformations at 1.5 GPa," J. Phys. Chem. B **103**, 1800–1804 (1999).

[70]M. Menon, K. R. Subbaswamy, and M. Sawtarie, "Structure and properties of C_{60} dimers by generalized tight-binding molecular dynamics," Phys. Rev. B **49**, 13966–13969 (1994).

[71]I. O. Bashkin, V. I. Rashchupkin, A. F. Gurov, A. P. Moravsky, O. G. Rybchenkot, and N. P. Kobelev, "A new phase transition in the T-P diagram of C_{60} fullerite," J. Phys.: Condens. Matter **6**, 7491 (1994).

[72]V. Agafonov, V. A. Davydov, L. S. Kashevarova, A. V. Rakhmanina, A. Kahn-Harari, P. Dubois *et al.*, "'Low-pressure' orthorhombic phase formed from pressure-treated C_{60}," Chem. Phys. Lett. **267**, 193–198 (1997).

[73]R. Moret, P. Launois, T. Wågberg, and B. Sundqvist, "Chain orientation and layer stacking in the high-pressure polymers of C_{60}: Single crystal studies," AIP Conf. Proc. **544**, 81–84 (2000).

[74]T. Wågberg, A. Soldatov, and B. Sundqvist, "Spectroscopic study of phase transformations between orthorhombic and tetragonal C_{60} polymers," Eur. Phys. J. B **49**, 59–65 (2006).

[75]V. A. Davydov, V. Agafonov, A. V. Dzyabchenko, R. Céolin, and H. Szwarc, "Packing models for high-pressure polymeric phases of C_{60}," J. Solid State Chem. **141**, 164–167 (1998).

[76]J. G. Hou, A. D. Zhao, T. Huang, and S. Lu, "C_{60}-based materials," ChemInform **36** (17) (2005).

[77]S. Okada and A. Oshiyama, "Electronic structure of metallic rhombohedral C_{60} polymers," Phys. Rev. B **68**, 235402 (2003).

[78]S. Yamanaka, A. Kubo, K. Inumaru, K. Komaguchi, N. S. Kini, T. Inoue *et al.*, "Electron conductive three-dimensional polymer of cuboidal C_{60}," Phys. Rev. Lett. **96**, 076602 (2006).

[79]K. P. Meletov, G. A. Kourouklis, J. Arvanitidis, K. Prassides, and Y. Iwasa, "Pressure-induced transformation and phonon modes of the two-dimensional rhombohedral polymer of C_{60}: A Raman spectroscopy," Phys. Rev. B **68**, 094103 (2003).

[80]J. M. Léger, J. Haines, V. A. Davydov, and V. Agafonov, "Irreversible amorphization of tetragonal two-dimensional polymeric C_{60} under high pressure," Solid State Commun. **121**, 241–244 (2002).

[81]K. P. Meletov, S. Assimopoulos, I. Tsilika, G. A. Kourouklis, J. Arvanitidis, S. Ves *et al.*, "High-pressure-induced metastable phase in tetragonal 2D polymeric C_{60}," Chem. Phys. Lett. **341**, 435–441 (2001).

[82]A. V. Talyzin and L. S. Dubrovinsky, "*In situ* Raman study of path-dependent C_{60} polymerization: Isothermal compression up to 32 GPa at 800 K," Phys. Rev. B **68**, 233207 (2003).

[83]W. Cui, M. Yao, S. Liu, F. Ma, Q. Li, R. Liu *et al.*, "A new carbon phase constructed by long-range ordered carbon clusters from compressing C_{70} solvates," Adv. Mater. **26**, 7257–7263 (2014).

[84]M. Yao, W. Cui, J. Xiao, S. Chen, J. Cui, R. Liu *et al.*, "Pressure-induced transformation and superhard phase in fullerenes: The effect of solvent intercalation," Appl. Phys. Lett. **103**, 071913 (2013).

[85]J. L. Hodeau, J. M. Tonnerre, B. Bouchet-Fabre, M. Núñez-Regueiro, J. J. Capponi, and M. Perroux, "High-pressure transformations of C_{60} to diamond and sp^3 phases at room temperature and to sp^2 phases at high temperature," Phys. Rev. B **50**, 10311–10314 (1994).

[86]F. Rachdi, C. Goze, L. Hajji, M. Núñez-Regueiro, L. Marques, J.-L. Hodeau *et al.*, "High resolution ^{13}C NMR studies of one- and two-dimensional polymerized C_{60} under high pressure," J. Phys. Chem. Solids **58**, 1645–1647 (1997).

[87]P.-A. Persson, U. Edlund, P. Jacobsson, D. Johnels, A. Soldatov, and B. Sundqvist, "NMR and Raman characterization of pressure polymerized C_{60}," Chem. Phys. Lett. **258**, 540–546 (1996).

[88]A. Rezzouk, Y. Errammach, F. Rachdi, V. Agafonov, and V. A. Davydov, "High-resolution ^{13}C NMR studies of the tetragonal two-dimensional polymerized C_{60} phase," Physica E **8**, 1–4 (2000).

[89]C. Goze, F. Rachdi, L. Hajji, M. Núñez-Regueiro, L. Marques, J.-L. Hodeau *et al.*, "High-resolution ^{13}C NMR studies of high-pressure-polymerized C_{60}: Evidence for the [2+2] cycloaddition structure in the rhombohedral two-dimensional C_{60} polymer," Phys. Rev. B **54**, R3676–R3678 (1996).

[90]K. Tanaka, Y. Matsuura, Y. Oshima, and T. Yamabe, "Electronic structure of a linear C_{60} polymer," Solid State Commun. **93**, 163–165 (1995).

[91]C. I. Frum, R. Engleman, Jr., H. G. Hedderich, P. F. Bernath, L. D. Lamb, and D. R. Huffman, "The infrared emission spectrum of gas-phase C_{60} (buckminsterfullerene)," Chem. Phys. Lett. **176**, 504–508 (1991).

[92]F. Zhang, C. Mihoc, F. Ahmed, C. Lathe, and E. Burkel, "Thermal stability of carbon nanotubes, fullerene and graphite under spark plasma sintering," Chem. Phys. Lett. **510**, 109–114 (2011).

[93]G. Wang, K. Komatsu, Y. Murata, and M. Shiro, "Synthesis and X-ray structure of dumb-bell-shaped C_{120}," Nature **387**, 583–586 (1997).

[94]P. Nagel, V. Pasler, S. Lebedkin, A. Soldatov, C. Meingast, B. Sundqvist *et al.*, "C_{60} one- and two-dimensional polymers, dimers, and hard fullerite: Thermal expansion, anharmonicity, and kinetics of depolymerization," Phys. Rev. B **60**, 16920–16927 (1999).

[95]Y. Saito, H. Shinohara, M. Kato, H. Nagashima, M. Ohkohchi, and Y. Ando, "Electric conductivity and band gap of solid C_{60} under high pressure," Chem. Phys. Lett. **189**, 236–240 (1992).

[96]M. Shiraishi, M. Ramm, and M. Ata, "The characterization of plasma-polymerized C_{60} thin films," Appl. Phys. A: Mater. Sci. Process. **74**, 613–616 (2002).

[97]T. L. Makarova, P. Scharff, B. Sundqvist, B. Narymbetov, H. Kobayashi, M. Tokumoto *et al.*, "Anisotropic metallic properties of highly - oriented rhombohedral C_{60} polymer," Synth. Met. **121**, 1099–1100 (2001).

[98]T. L. Makarova, B. Sundqvist, P. Scharff, M. E. Gaevski, E. Olsson, V. A. Davydov *et al.*, "Electrical properties of two-dimensional fullerene matrices," Carbon **39**, 2203–2209 (2001).

[99]A. V. Okotrub, V. V. Belavin, L. G. Bulusheva, V. A. Davydov, T. L. Makarova, and D. Tománek, "Electronic structure and properties of rhombohedrally polymerized C_{60}," J. Chem. Phys. **115**, 5637–5641 (2001).

[100]S. G. Buga, V. D. Blank, G. A. Dubitsky, L. Edman, X.-M. Zhu, E. B. Nyeanchi *et al.*, "Semimetallic and semiconductor properties of some superhard and ultrahard fullerites in the range 300–2 K," J. Phys. Chem. Solids **61**, 1009–1015 (2000).

[101]J. Laranjeira, L. Marques, N. M. Fortunato, M. Melle-Franco, K. Strutyński, and M. Baroso, "Three-dimensional C_{60} polymers with ordered binary-alloy-type structures," Carbon **137**, 511–518 (2018).

[102]J. Laranjeira, L. Marques, M. Mezouar, M. Melle-Franco, and K. Strutyński, "Bonding frustration in the 9.5 GPa *fcc* polymeric C_{60}," Phys. Status Solidi Rapid Res. Lett. **11**, 1700343 (2017).

[103]A. Soldatov and O. Andersson, "Thermal conductivity of pressure polymerized C_{60}," Appl. Phys. A **64**, 227–229 (1997).

[104]D. Liu, M. Yao, L. Wang, Q. Li, W. Cui, B. Liu *et al.*, "Pressure-induced phase transitions of C_{70} nanotubes," J. Phys. Chem. C **115**, 8918–8922 (2011).

[105]B. Sundqvist, "Intermolecular bonding in C_{70} at high pressure and temperature," Carbon **125**, 258–268 (2017).

[106]H. Kawamura, M. Kobayashi, Y. Akahama, H. Shinohara, H. Sato, and Y. Saito, "Orientational ordering in solid C_{70} under high pressure," Solid State Commun. **83**, 563–565 (1992).

[107]C. Christides, M. Thomas, T. J. S. Dennis, and K. Prassides, "Pressure and temperature evolution of the structure of solid C_{70}," Europhys. Lett. **22**, 611–618 (1993).

[108]A. V. Soldatov, G. Roth, A. Dzyabchenko, D. Johnels, S. Lebedkin, C. Meingast, M. Haluska, H. Kuzmany *et al.*, "Topochemical polymerization of C_{70} controlled by monomer crystal packing," Science **293**, 680–683 (2001).

[109]V. D. Blank, N. R. Serebryanaya, G. A. Dubitsky, S. G. Buga, V. N. Denisov, B. N. Mavrin *et al.*, "Polymerization and phase diagram of solid C_{70} after high-pressure-high-temperature treatment," Phys. Lett. A **248**, 415–422 (1998).

[110]V. D. Blank, B. A. Kulnitskiy, and O. M. Zhigalina, "Dimerisation and polymerisation of C_{70} after thermobaric," Carbon **38**, 2051–2054 (2000).

[111]L. Marques, Y. Skorokhod, and R. Soares, "Extended polymerization in ABC-stacked C_{70} fullerite," Carbon **82**, 599–603 (2015).

[112]L. Marques, Y. Skorokhod, and R. Soares, "A new fullerene network phase obtained from C_{70} at high-pressure and high-temperature," Phys. Status Solidi Rapid Res. Lett. **9**, 535–538 (2015).

[113]A. Demortier, R. Doome, A. Fonseca, and J. B. Nagy, "Study of the anomalous solubility behavior of solutions saturated with fullerenes by ^{13}C-NMR," Magn. Reson. Colloid Interface Sci. **76**, 513–518 (2002).

[114]R. M. Fleming, A. R. Kortan, B. Hessen, T. Siegrist, F. A. Thiel, P. Marsh *et al.*, "Pseudotenfold symmetry in pentane-solvated C_{60} and C_{70}," Phys. Rev. B **44**, 888–891 (1991).

[115]F. Michaud, M. Barrio, D. O. López, J. Ll. Tamarit, V. Agafonov, S. Toscani *et al.*, "Solid-state studies on a C_{60} solvate grown from 1,1,2-trichloroethane," Chem. Mater. **12**, 3595–3602 (2000).

[116]M. Barrio, D. O. López, J. Ll. Tamarit, P. Espeau, and R. Céolin, "Solid-state studies of C_{60} solvates formed in the C_{60}-$BrCCl_3$ system," Chem. Mater. **15**, 288–291 (2003).

[117]R. Céolin, J. Ll. Tamarit, M. Barrio, D. O. López, P. Espeau, H. Allouchi *et al.*, "Solid state studies of the C_{60}. $2(CH_3)CCl_3$ solvate," Carbon **43**, 417–424 (2005).

[118]S. Toscani, H. Allouchi, J. Ll. Tamarit, D. O. López, M. Barrio, V. Agafonov *et al.*, "Decagonal C_{60} crystals grown from n-hexane solutions: Solid-state and aging studies," Chem. Phys. Lett. **330**, 491–496 (2000).
[119]S. M. Gorun, K. M. Creeqan, R. D. Sherwood, D. M. Cox, V. W. Day, C. S. Day *et al.*, "Solvated C_{60} and C_{60}/C_{70} and the low-resolution single crystal X-ray structure of C_{60}," J. Chem. Soc., Chem.Commun. **21**, 1556–1558 (1991).
[120]M. V. Korobov, E. B. Stukalin, A. L. Mirakyan, I. S. Neretin, Y. L. Slovokhotov, A. V. Dzyabchenko *et al.*, "New solid solvates of C_{60} and C_{70} fullerenes: The relationship between structures and lattice energies," Carbon **41**, 2743–2755 (2003).
[121]R. Céolin, J. Ll. Tamarit, M. Barrio, D. O. López, S. Toscani, H. Allouchi *et al.*, "Solid-state studies on a cubic 1:1 solvate of C_{60} grown from dichloromethane and leading to another hexagonal C_{60} polymorph," Chem. Mater. **13**, 1349–1355 (2001).
[122]P. Espeau, M. Barrio, D. O. López, J. Ll. Tamarit, R. Céolin, H. Allouchi *et al.*, "Phase equilibria in the C_{60}^{+} ferrocene system and solid-state studies of the C_{60}•2ferrocene solvate," Chem. Mater. **14**, 321–326 (2002).
[123]R. Świetlik, P. Byszewski, and E. Kowalska, "Interactions of C_{60} with organic molecules in solvate crystals studied by infrared spectroscopy," Chem. Phys. Lett. **254**, 73–78 (1996).
[124]A. Talyzin and U. Jansson, "C_{60} and C_{70} solvates studied by Raman spectroscopy," J. Phys. Chem. B **104**, 5064–5071 (2000).
[125]E. Mitsari, M. Romanini, N. Qureshi, J. Ll. Tamarit, M. Barrio, and R. Macovez, "C_{60} solvate with (1,1,2)-trichloroethane: Dynamic statistical disorder and mixed conformation," J. Phys. Chem. C **120**, 12831–12839 (2016).
[126]A. K. Gangopadhyay, J. S. Schilling, M. De. Leo, W. E. Buhro, K. Robinson, and T. Kowalewski, "Synthesis and characterization of $C_{60}\{CCl_4\}_{10}$," Solid State Commun. **96**, 597–600 (1995).
[127]A. Graja and R. Świetlik, "Temperature study of IR spectra of some C_{60} compounds," Synth. Met. **70**, 1417–1418 (1995).
[128]C. Park, E. Yoon, M. Kawano, T. Joo, and H. C. Choi, "Self-Crystallization of C_{70} cubes and remarkable enhancement of photoluminescence," Angew. Chem., Int. Ed. **49**, 9670–9675 (2010).
[129]M. Du, M. Yao, S. Chen, B. Sundqvist, X. Yang, R. Liu *et al.*, "Effect of C_{70} rotation on the photoluminescence spectra of compressed C_{70}*mesitylene," J. Raman Spectrosc. **48**, 437–442 (2016).
[130]C. A. Kuntscher, S. Frank, K. Kamarás, G. Klupp, É. Kováts, S. Pekker *et al.*, "Pressure-dependent infrared spectroscopy on the fullerene rotor-stator compound C_{60}-C_8H_8," Phys. Status Solidi B **243**, 2981–2984 (2006).
[131]D. Liu, L. Wang, W. Cui, M. Yao, Q. Li, Z. Li *et al.*, "Synthesis and solid-state studies of self-assembled C_{60} microtubes," Diamond Relat. Mater. **20**, 178–182 (2011).
[132]K. P. Meletov and D. V. Konarev, "Raman study of the pressure-induced phase transitions in the molecular donor-acceptor complex $\{Pt(dbdtc)_2\}C_{60}$," Chem. Phys. Lett. **553**, 21–25 (2012).
[133]K. P. Meletov and D. V. Konarev, "Raman study of the pressure-induced charge transfer transition in the neutral donor-acceptor complexes $\{Ni(nPr_2dtc)_2\}(C_{60})_2$ and $\{Cu(nPr_2dtc)_2\}(C_{60})_2$," Fullerenes, Nanotubes, Carbon Nanostruct. **20**, 336–340 (2012).
[134]Y. Akahama, M. Kobayashi, H. Kawamura, H. Shinohara, H. Sato, and Y. Saito, "Electrical resistance of iodine-doped C_{60} under high pressure," Solid State Commun. **82**, 605–607 (1992).
[135]W. Cui, M. Yao, Z. Yao, F. Ma, Q. Li, R. Liu *et al.*, "Reversible pressure-induced polymerization of $Fe(C_5H_5)_2$ doped C_{70}," Carbon **62**, 447–454 (2013).
[136]K. Thirunavukkuarasu, C. A. Kuntscher, B. J. Nagy, I. Jalsovszky, G. Klupp, K. Kamarás *et al.*, "Orientational ordering and intermolecular interactions in the rotor-stator compounds C_{60}•C_8H_8 and C_{70}•C_8H_8 studied under pressure," J. Phys. Chem. C **112**, 17525–17532 (2008).
[137]A. V. Talyzin, L. S. Dubrovinsky, and U. Jansson, "High pressure Raman study of $C_{60}S_{16}$," Solid State Commun. **123**, 93–96 (2002).
[138]K. Mizoguchi, M. Takei, H. Sakamoto, T. Kawamoto, M. Tokumoto, A. Omerzu *et al.*, "Uniaxial strain study in purely organic ferromagnet α-TDAE-C_{60}-Mechanism and structure," Polyhedron **24**, 2173–2175 (2005).
[139]K. Mizoguchi, M. Machino, H. Sakamoto, T. Kawamoto, M. Tokumoto, A. Omerzu *et al.*, "Pressure effect in TDAE-C_{60} ferromagnet: Mechanism and polymerization," Phys. Rev. B **63**, 140417 (2001).
[140]W. Cui, M. Yao, D. Liu, Q. Li, R. Liu, B. Zou *et al.*, "Reversible polymerization in doped fullerides under pressure: The case of $C_{60}(Fe(C_5H_5)_2)_2$," J. Phys. Chem. B **116**, 2643–2650 (2012).
[141]K. Kato, H. Murata, H. Gonnokami, and M. Tachibana, "Polymerization in ferrocene-doped C_{60} nanosheets under high pressure and light irradiation," Carbon **107**, 622–628 (2016).
[142]M. Du, M. Yao, J. Dong, P. Ge, Q. Dong, É. Kováts *et al.*, "New ordered structure of amorphous carbon clusters induced by fullerene-cubane reactions," Adv. Mater. **30**, 1706916 (2018).
[143]M. Yao, W. Cui, M. Du, J. Xiao, X. Yang, S. Liu *et al.*, "Tailoring building blocks and their boundary interaction for the creation of new, potentially superhard, carbon materials," Adv. Mater. **27**, 3962–3968 (2015).
[144]D. Liu, M. Yao, Q. Li, W. Cui, L. Wang, Z. Li *et al.*, "*In situ* Raman and photoluminescence study on pressure-induced phase transition in C_{60} nanotubes," J. Raman Spectrosc. **43**, 737–740 (2012).
[145]B. W. Smith, M. Monthioux, and D. E. Luzzi, "Encapsulated C_{60} in carbon nanotubes," Nature **396**, 323–324 (1998).
[146]B. W. Smith and D. E. Luzzi, "Formation mechanism of fullerene peapods and coaxial tubes: A path to large scale synthesis," Chem. Phys. Lett. **321**, 169–174 (2000).
[147]S. Okada, S. Saito, and A. Oshiyama, "Energetics and electronic structures of encapsulated C_{60} in a carbon nanotube," Phys. Rev. Lett. **86**, 3835–3838 (2001).
[148]M. Hodak and L. A. Girifalco, "Systems of C_{60} molecules inside (10,10) and (15,15) nanotube: A Monte Carlo study," Phys. Rev. B **68**, 085405 (2003).
[149]M. Chorro, J. Cambedouzou, A. Iwasiewicz-Wabnig, L. Noé, S. Rols, M. Monthioux *et al.*, "Discriminated structural behaviour of C_{60} and C_{70} peapods under extreme conditions," Europhys. Lett. **79**, 56003 (2007).
[150]X. Yang, M. Yao, X. Wu, S. Liu, S. Chen, K. Yang *et al.*, "Novel superhard sp^3 carbon allotrope from cold-compressed C_{70} peapods," Phys. Rev. Lett. **118**, 245701 (2017).
[151]Q. Li, Y. Ma, A. R. Oganov, H. B. Wang, H. Wang, Y. Wang *et al.*, "Superhard monoclinic polymorph of carbon," Phys. Rev. Lett. **102**, 175506 (2009).
[152]M. Kosaka, K. Tanigaki, K. Prassides, S. Margadonna, A. Lappas, C. M. Brown *et al.*, "Superconductivity in Li_xCsC_{60} fullerides," Phys. Rev. B **59**, R6628 (1999).
[153]S. Margadonna and K. Prassides, "Recent advances in fullerene superconductivity," J. Solid State Chem. **168**, 639–652 (2002).
[154]K. Tanigaki, T. W. Ebbesen, S. Saito, J. Mizuki, S. Tsai, Y. Kubo *et al.*, "Superconductivity at 33 K in $Cs_xRb_yC_{60}$," Nature **352**, 222–223 (1991).
[155]P. W. Stephens, G. Bortel, G. Faigel, M. Tegze, A. Jánossy, S. Pekker *et al.*, "Polymeric fullerene chains in RbC_{60} and KC_{60}," Nature **370**, 636–639 (1994).
[156]R. Poloni, D. Machon, M. V. Fernandez-Serra, S. Le. Floch, S. Pascarelli, G. Montagnac *et al.*, "High-pressure stability of Cs_6C_{60}," Phys. Rev. B **77**, 125413 (2008).
[157]R. Poloni, G. Aquilanti, P. Toulemonde, S. Pascarelli, S. Le. Floch, D. Machon *et al.*, "High-pressure phase transition in Rb_6C_{60}," Phys. Rev. B **77**, 205433 (2008).
[158]M. Riccò, M. Belli, M. Mazzani, D. Pontiroli, D. Quintavalle *et al.*, "Superionic Conductivity in the Li_4C_{60} fulleride polymer," Phys. Rev. Lett. **102**, 145901 (2009).
[159]M. Yao, T. Wågberg, and B. Sundqvist, "Effect of high pressure on electrical transport in the Li_4C_{60} fulleride polymer from 100 to 400 K," Phys. Rev. B **81**, 155441 (2010).
[160]M. Yao, T. Wågberg, and B. Sundqvist, "Electrical transport properties of Na_2C_{60} under high pressure," Phys. Rev. B **80**, 115405 (2009).
[161]V. D. Blank, S. G. Buga, N. R. Serebryanaya, V. N. Denisov, G. A. Dubitsky, A. N. Ivlev *et al.*, "Ultrahard and superhard carbon phases produced from C_{60} by heating at high pressure: Structural and Raman studies," Phys. Lett. A **205**, 208–216 (1995).